## 4.4 ANALYSIS OF SPATIAL REPRESENTATIVENESS OF URBAN MONITORING STATIONS USING STEADY CFD-RANS SIMULATIONS

J. L. Santiago[1*], M. A. Parra[2], A. Martilli[1], F. Martín[1], J. M. Santamaría[2]
[1]Environmental Department, CIEMAT (Center for Research on Energy, Environment and Technology). Madrid, Spain.
[2] Laboratorio Integrado de Calidad Ambiental (LICA), Departamento de Química y Edafología, Facultad de Ciencias, Universidad de Navarra. Pamplona, Navarra, Spain.

### 1. INTRODUCTION

Urban air quality assessment is an important task, complicated by the heterogeneities induced by urban morphology on the atmospheric features in the urban canopy layer. A network of urban monitoring stations, as used in most European cities, is often not enough because the spatial representativeness of point measurements is limited due to these heterogeneities. Hence, urban modeling can be a useful tool to complement experimental data from an urban air quality network of stations.

Computational Fluid Dynamic (CFD) models solve flow and dispersion around the buildings explicitly and can provide detailed flow and dispersion patterns inside urban zones (streets, squares,...). However, the computational time required for this type of simulations is high and it is not possible to perform an unsteady CFD simulation during large time periods in order to get daily, monthly or annual averaged concentration distributions which are often required by regulatory purposes. To solve this problem, we propose a methodology based on a set of steady CFD simulations with different inlet wind directions. These simulations are based on Reynolds-averaged Navier-Stokes equations (RANS).

The emissions are modeled with a line source inside each street. In order to compute the total concentration, the predominant wind direction at each hour is taken into account, together with some factors to modulate the simulated concentrations (wind speed, hourly number of cars, and length of streets).

This methodology is applied to a real case (a central square in Pamplona, Spain) and it has been evaluated against experimental measurements (Parra et al., 2010).

* *Corresponding author address:* Jose Luis Santiago, CIEMAT, Environmental Department, Av. Complutense 22, 28040, Madrid, Spain; email: jl.santiago@ciemat.es

The assessment of air quality is usually made according to urban station measurements but it is also important to have an estimate of the concentration around the station to complement its measured data. Hence, we analyze the modeled concentration at the station location in comparison with the concentration in its surroundings in order to estimate the spatial representativeness of the urban monitoring station.

The main objectives of this work are:

a) To describe a methodology to use CFD-RANS simulations to obtain pollutant concentrations during large time periods inside urban environments.

b) To apply this methodology to a real case.

c) To study the representativeness of an urban monitoring station in a real case.

### 2. DESCRIPTION OF METHODOLOGY

The objective of this methodology is to evaluate the air quality inside a real urban area by means of CFD simulations. Due to computational restrictions, unsteady CFD simulations during a simulation time period of weeks or months can not be performed at affordable time. In order to solve this problem a methodology using steady CFD simulations for several wind directions was developed (Parra et al., 2010).

A steady CFD simulation for every wind direction sector (16 different wind directions: N, NNE, NE, ...) is considered. In each simulation several passive tracers are released, one for each street. Based on the linearity of model equations we can compute a concentration proportional to the real one at time *t* using equation 1.

$$C_{\mathrm{Real}}(t) \propto C_{\mathrm{computed}}(Sector(t)) = \sum_i C_i(Sector(t)) \cdot \frac{L_i}{Vsource_i} \cdot N_i(t) \cdot \frac{1}{v_{in}(t)} \qquad (1)$$

where $i$ is each street (each tracer used), *Sector*($t$) is the wind direction sector at $t$, $C_i$(*Sector*($t$)) is the concentration computed for *Sector*($t$) for a given emission from street $i$ and for a given inlet wind speed, $L_i$ is the length of the street $i$, $Vsource_i$ is the volume of the row of computational cells where emission of the street $i$ is located, $N_i(t)$ is the number of cars per unit time in street i, and $v_{in}$ is the inlet wind speed.

The meaning of equation 1 is the following. At time $t$ we observe the wind direction and use the results of CFD simulations for this wind sectors. Then the contributions of each tracer (modulated by $\frac{L_i}{Vsource_i} \cdot N_i(t)$ and $\frac{1}{v_{in}(t)}$) are added obtaining a concentration proportional to the real. Note that the real emissions are unknown and the emissions in CFD simulations are considered the same inside each street. Therefore, the factors $\frac{L_i}{Vsource_i} \cdot N_i(t)$ are used to take into account the different emissions inside each street. The factor $\frac{1}{v_{in}(t)}$ is used because the concentration is inversely proportional to inlet wind speed and for the real case the speed could be different to the inlet wind speed used in CFD simulations.

In this calculation the following assumptions have been made:

a) Pollutants must be non-reactive or at least for the time period studied pollutants should be little influenced by atmospheric chemistry (e.g. some photochemically pollutants in winter, Sillman, 1999; Atkinson, 2000).
b) Thermal effects are negligible in comparison with dynamical effects.
c) Emissions inside each street at a selected hour are proportional to traffic intensity at that hour.
d) Tracer concentration at a certain hour only depends on emissions and meteorological conditions at that hour.

More details about the methodology can be found in Parra et al. (2010).

## 3. APLICATION TO A REAL CASE

The methodology presented above has been applied to a square in Pamplona, a medium city of Spain. This square is surrounded by 15 m-height buildings.

CFD simulations were based on Reynolds-averaged Navier-Stokes (RANS) equations. The turbulent closure used was standard *k-e*. The tracers were simulated by means of a transport equation for passive scalar (Santiago et al, 2007; Parra et al., 2010). An irregular computational mesh with $3.5 \cdot 10^6$ cells approximately was used. The cell size was smaller close to buildings. We have a resolution of 2 m in X- and Y-direction and 1.5 m in Z-direction. Symmetry boundary conditions were used at the top and standard wall functions at solid boundaries (buildings and ground). Figure 1 shows the real geometry, modeled geometry and a detail of the computational mesh. Simulations for 16 wind directions (one for each wind sector: N, NNE, NE, ...) were performed.

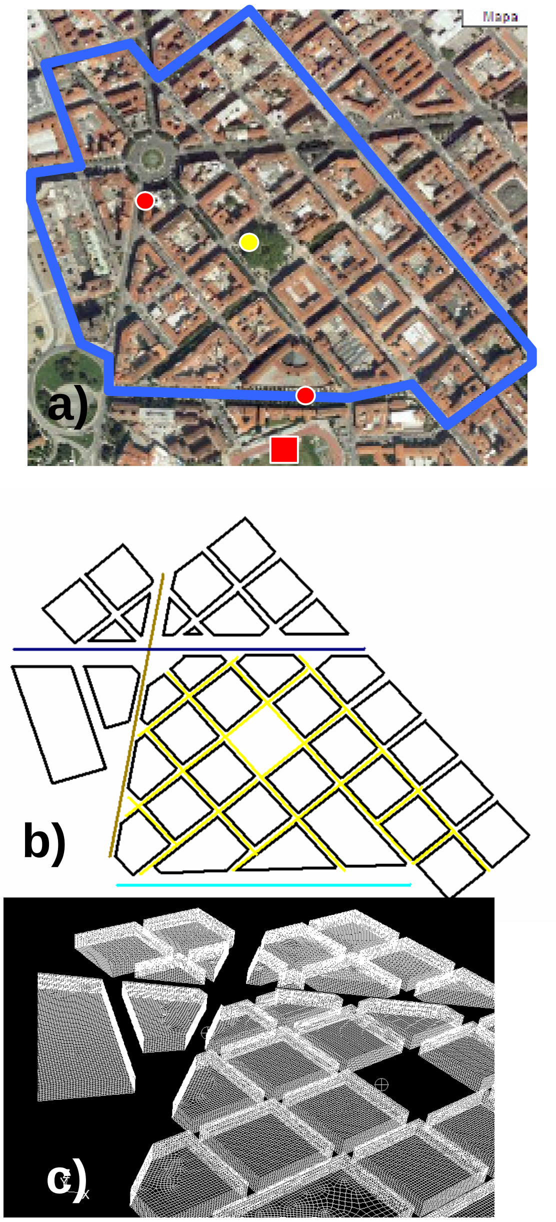


**Figure 1.** Plan view of a) real geometry, Circles are location of passive samplers (yellow is urban monitoring station). Square is meteorological tower. b) modeled geometry. Color lines are locations of different emissions. c) detail of the 3D computational mesh.

An evaluation of the results of methodology was performed by comparing with experimental measurements. The time period of January and February 2007 was chosen because pollutants are little affected by atmospheric chemistry in winter (Sillman, 1999; Atkinson, 2000). Temporal evolution of hourly mean concentration of $NO_x$ and PM10 from the monitoring station at 'Plaza de la Cruz' (yellow circle in Fig. 1a) were compared. Temporal series of concentrations of PM10 normalized by the concentration averaged over the selected time period in this station are shown in Fig.2. A suitable agreement is observed. The highest differences are for cases where wind speed is very low.

In addition to analyze the representativeness of the experimental measurements, this methodology can also be useful to urban planning (re-organization of traffic, changes in buildings layouts,...).

## 4. REPRESENTATIVENESS OF URBAN MONITORING STATION

Usually air quality is evaluated by means of measurements from monitoring stations. However, in urban environment the representativeness of measurements in only one point is limited to a small zone. This is due to the complex flow over the streets that transports pollutants and produces strong heterogeneities in the concentration patterns. Hence, the network of monitoring can not be dense enough to provide representative concentration of every zone in the city. To illustrate this issue, contour maps at $z$ = 3 m for the same emissions and meteorological conditions except for wind direction are shown in Fig. 4. We can observe that the value of the monitoring station is very different from the concentrations in other near points. In WNW case, the values around the monitoring station are lower than that computed at that point. In NE case, it is the other way around.

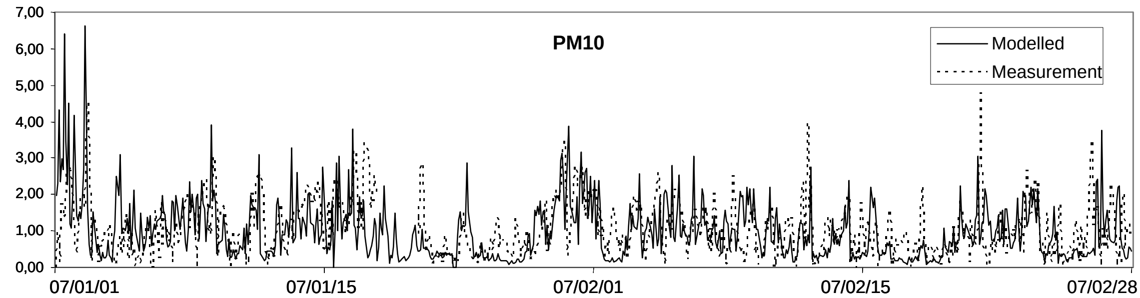


**Figure 2.** Temporal series of measured and computed PM10 concentrations.

In addition, experimental two-weeks averaged concentrations of several pollutants ($NO_2$ and BTEX) in three sampling points (circles in Fig. 1a) from four sampling campaigns (Parra et al., 2009; Parra et al., 2010) are used in the comparison. For example, modeled vs experimental concentrations of $NO_2$ normalized by the concentration averaged over the selected time period (January and February) in the three sampling points are plotted in Fig. 3. A high correlation was found ($R^2$ = 0.95).

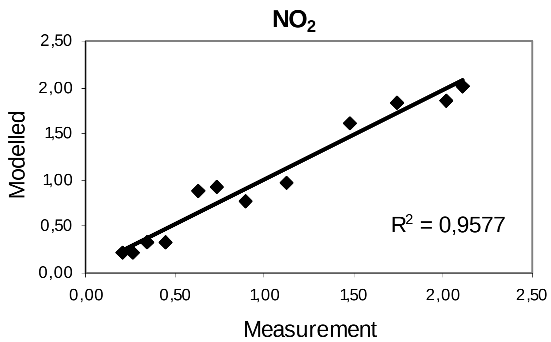


**Figure 3.** Linear regression between modelled and experimental two-weeks averaged concentration of $NO_2$.

These results show a suitable performance of the methodology based on CFD-RANS simulations.

In this study, we present the modeling and in particular the methodology developed as a useful tool to complement measurements from urban monitoring stations.

Firstly, we analyze the value of computed concentrations at monitoring position in comparison with the values obtained around this location. For this purpose concentration values are normalized by the value at monitoring location and analyze the maximum concentration obtained at different distances from the station. Table 1 shows some numerical results and Fig. 4 shows the contour maps normalized for NE and NNW.

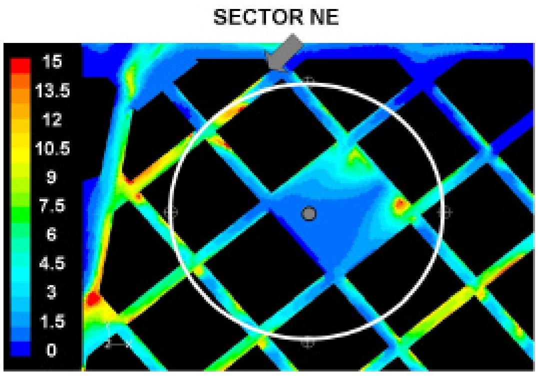


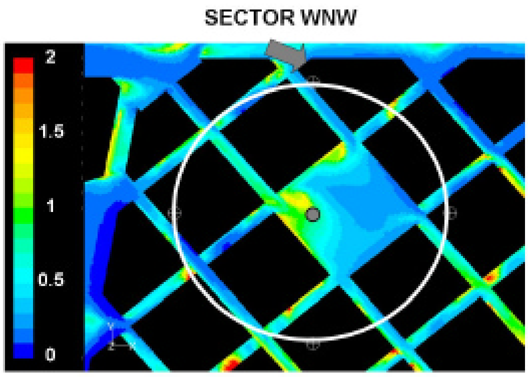


**Figure 4.** Concentration normalized by the computed concentration at monitoring location. White line indicates 100 m further from the station location (grey circle).

These results show that very different concentrations than those at the station (even 10 times higher) can be found for distance lower than 100 m from station.

Next step of this study is to consider the real meteorology (frequency and mean wind speed corresponding to each sector). Note that the concentration is inversely proportional to wind speed. Meteorological conditions are computed for the time period January - February 2007 and from 8h to 20h of each day (where the main emissions are released). Table 2 indicates these data.

For some wind sectors (N, NNE, NW and NNW) there are locations close to the station with concentration values of several times higher than the station concentration. However, mean wind speed for these sectors is relatively high and differences in absolute values are small. Note that these sectors cover 40% of the total cases. For other sectors like WNW, W and SW, the wind speed is low and concentration is high but the monitoring station is located close to a maximum and the concentration around it is not much higher. On the other hand, for ESE or SE sectors, model results show regions with high concentration, even if the concentration at the measurement point is low. This is another evidence that using point measurements to assess air quality may lead to erroneous conclusions.

| SECTOR | $C_{max}/C_{sta}$ (R=100) | $d_{max}$ (R=100) | $C_{max}/C_{sta}$ (R=75) | $d_{max}$ (R=75) | $C_{max}/C_{sta}$ (R=50) | $d_{max}$ (R=50) |
|---|---|---|---|---|---|---|
| **N** | 10.95 | 89.92 | 6.71 | 74.47 | 5.51 | 3.11 |
| **NNE** | 8.26 | 60.09 | 8.26 | 60.09 | 7.91 | 36.77 |
| **NE** | 15.43 | 96.67 | 14.18 | 70.44 | 12.50 | 48.27 |
| **ENE** | 9.81 | 93.57 | 7.80 | 71.62 | 5.04 | 49.23 |
| **E** | 8.75 | 69.21 | 8.75 | 69.21 | 4.95 | 48.66 |
| **ESE** | 5.94 | 81.95 | 4.92 | 52.97 | 4.32 | 49.08 |
| **ES** | 15.44 | 97.95 | 7.50 | 74.53 | 4.65 | 17.42 |
| **SSE** | 9.28 | 94.48 | 7.83 | 66.75 | 6.67 | 49.09 |
| **S** | 8.27 | 98.42 | 5.49 | 69.83 | 4.31 | 13.89 |
| **SSW** | 4.58 | 98.41 | 3.70 | 15.78 | 3.70 | 15.78 |
| **SW** | 3.10 | 79.50 | 3.05 | 74.46 | 2.85 | 17.63 |
| **WSW** | 4.26 | 90.59 | 4.13 | 22.82 | 4.13 | 22.82 |
| **W** | 1.87 | 5.02 | 1.87 | 5.02 | 1.87 | 5.02 |
| **WNW** | 2.29 | 90.37 | 1.59 | 20.91 | 1.59 | 20.91 |
| **NW** | 7.71 | 11.34 | 7.71 | 11.34 | 7.71 | 11.34 |
| **NNW** | 6.09 | 77.96 | 5.11 | 5.74 | 5.11 | 5.74 |

**Table 1.** Normalized value and position of concentration maxima inside circles with radius of 100, 75 and 50 m around station location (height = 3 m). $C_{max}$, $C_{sta}$ are maximum and station concentration respectively. $d_{max}$ is distance from station to maximum.

| Sectors | Frequency (%) | Mean wind speed (m/s) |
|---|---|---|
| N | 11.34 | 3.57 |
| NNE | 4.45 | 2.71 |
| NE | 2.70 | 1.33 |
| ENE | 5.67 | 1.38 |
| E | 7.42 | 1.15 |
| ESE | 6.07 | 0.97 |
| SE | 9.18 | 1.03 |
| SSE | 6.61 | 2.89 |
| S | 6.61 | 1.13 |
| SSW | 6.34 | 1.61 |
| SW | 5.40 | 1.54 |
| WSW | 5.40 | 1.42 |
| W | 3.37 | 1.54 |
| WNW | 2.70 | 1.68 |
| NW | 6.07 | 2.30 |
| NNW | 10.66 | 3.43 |

**Table 2.** Meteorological conditions during January-February 2007 from 8h to 20h.

Finally, the representativeness of the station is analyzed in terms of mean concentrations. With the methodology developed, mean concentration is computed for the time period above mentioned taking into account the contribution of every wind direction as a function of wind speed and frequency. Figure 5 shows mean concentration map ($z$ = 3 m) normalized by mean concentration at the station location. White and grey contours indicate concentration similar to that obtained at station (1 ± 20%).

Similar values to that obtained at station position are only located in a donut-shape part of the square. Note that the differences between station concentration and concentration around it are notably smaller for mean values. Hypothetical locations of the new monitoring stations can be also studied. For example, we analyze cases where the station would be located at other zone of the square and in a nearby street (Fig. 6 and 7). We can observe that depending on the station location its concentration value is representative of concentration in different zones.

**5. CONCLUSIONS**

The main conclusions are the followings:

a) The methodology presented has reproduced with a suitable agreement experimental measurements.

b) This methodology has been applied to study the representativeness of monitoring stations.

c) Point measurements are insufficient to assess air quality over a wide urban zone. For this purpose, numerical modeling is a useful tool in order to give more information about pollutant distribution.

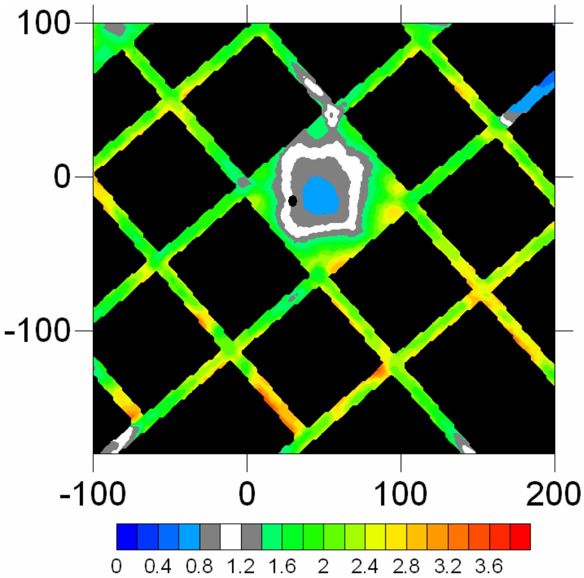


**Figure 5.** Mean concentration map normalized by concentration at station location (black dot).

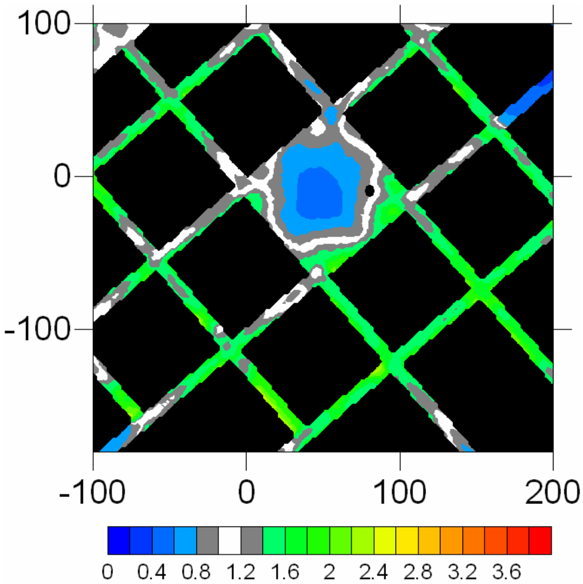


**Figure 6.** Same as Fig. 5 but for a hypothetical situation where station location has been changed (black dot).

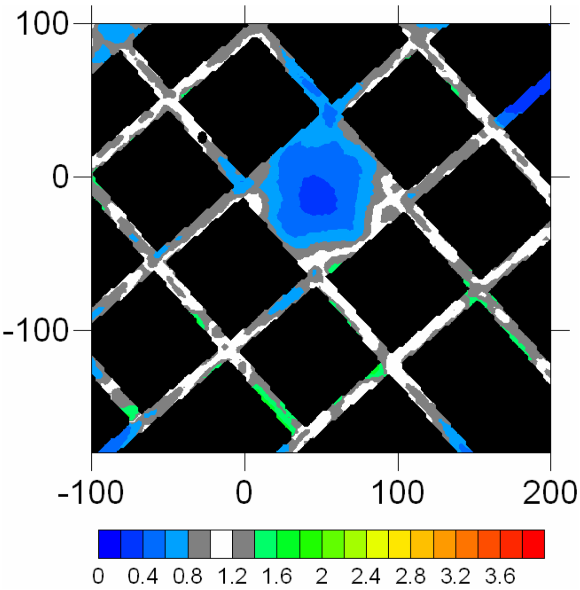


**Figure 7.** Same as Fig. 5 but for a hypothetical situation where station location has been changed (black dot).

## ACKNOWLEDGEMENTS

Authors would like to thank the local authorities for their collaboration and for the transferring of Pamplona traffic data, the Government of Navarra for pollutants and meteorological data and 'Fundación CAN' for the concession of a research grant to M.A. Parra. The modeling exercises of this study have been also partially supported by the Spanish Ministry of Environment, Marine and Rural Affairs.

## REFERENCES

Atkinson, R., 2000. Atmospheric chemistry of VOCs and $NO_x$. *Atmos. Environ.*, 34, 2063-2101.

Parra, M. A., Elustondo, D., Bermejo, R., Santiamaría, J. M., 2009. Ambient air levels of volatile organic compounds (VOC) and nitrogen dioxide (NO2) in a medium size city in Northern Spain. *Sci. Total Environ.*, 407, 999-1009.

Parra, M. A., Santiago, J. L., Martín, F., Martilli, A., Santamaría, J. M., 2010: A methodology to urban air quality assessment during large time periods of winter using computational fluid dynamic models. *Atmos. Environ.*, 44, 2089-2097.

Santiago, J. L., Martilli, A., Martín, F., 2007. CFD simulation of airflow over a regular array of cubes. Part I: three-dimensional simulation of the flow and validation with wind tunnel measurements. *Boundary-Layer Meteorol.*, 122, 609-634.

Sillman, S., 1999. The relation between ozone, $NO_x$ and hydrocarbons in urban and polluted rural environments. *Atmos. Environ.*, 33, 1821-1845.